Construction and Building Materials 384 (2023) 131439

Contents lists available at ScienceDirect

Construction and Building Materials

journal homepage: www.elsevier.com/locate/conbuildmat

A stress–temperature superposition approach to study the nonlinear resilient behavior of cold recycled mixtures (CRM) with active filler addition

Pablo Orosa [a,b,*], Ignacio Pérez [a], Ana R. Pasandín [a], John E. Haddock [b]

[a] E. T. S. de Ingeniería de Caminos, Canales y Puertos and CITEEC, Universidade da Coruña, A Coruña, Spain
[b] Lyles School of Civil Engineering, Purdue University, West Lafayette, IN, USA

ARTICLE INFO

Keywords:
Cold recycling mix
Bitumen emulsion
Reclaimed asphalt pavement
Triaxial testing
Resilient modulus
Active filler

ABSTRACT

The asphalt paving sector is currently embracing and enhancing cold mixture technologies to reduce carbon emissions and decarbonize its operations. Cold recycled mixtures (CRM) have proven to be a promising alternative in road construction and rehabilitation, becoming a primary research focus. This study evaluates the effects on compactability and volumetric properties of adding 1% Portland cement or 1% hydrated lime to CRM made with 100% reclaimed asphalt pavement and bitumen emulsion. Dynamic triaxial tests with different confinement pressures (ranging from 20 to 200 kPa) and temperatures (5, 15, 25, and 35 °C) were used to determine the influence of these active filler additions on the resilient modulus (*Mr*) of the mixtures. All the mixtures exhibited increased *Mr* values at lower temperatures and reduced stress–dependency. Cement addition had the most favorable effect on compactability, reducing the necessary compaction energy, while mixtures with hydrated lime had more substantial increases in *Mr* and reduced stress dependencies. Finally, the results were analyzed by plotting master curves using a proposed novel approach called Stress–Temperature Superposition Principle (STSP), which allows for simpler and more straightforward analyses.

1. Introduction

The current challenge posed by global warming and the need to reduce CO_2 emissions has led to a paradigm shift for many industries, which have had to reconsider many of their working practices [1]. Research and implementation of cold technologies are currently being promoted within the paving sector, thus achieving a degree of decarbonisation of its operations. A rehabilitation technique with great potential that meets these characteristics is cold recycling (CR), either in situ, known as cold in-place recycling or CIR [2,3], or in plant, known as cold central plant recycling (CCPR) [4,5].

Cold recycled mixtures (CRM) primarily consist of a recycled aggregate from milling deteriorated roads, known as reclaimed asphalt pavement (RAP), and a bituminous binder. This bituminous binder is usually in the form of an emulsion or foam so that it can be mixed without heating. An important additional component is the water, which is necessary to facilitate the mixing, extension, and compaction processes [6]. Furthermore, adding a specific content of active filler, such as cement, is common when aiming to improve the mechanical performance of CRM [7]. However, each active filler has a different effect, and so far, it is not completely clear which is the optimum dosage or filler type for CRM, so the content is usually limited, avoiding potential problems such as loss of flexibility or appearance of brittleness [7].

In contrast to asphalt concrete or hot mix asphalt (HMA), cold mix asphalt (CMA) with RAP presents a different mechanical behavior. While HMA are continuously bound materials, with a bitumen film coating all aggregates, CRM are half-bonded materials (Fig. 1), owing to the reduced binder content and the presence of water as one of the main constituents, which eventually evaporates after curing. Similar to all bituminous materials, CRM exhibit viscoelastic mechanical behavior (frequency- and temperature-dependent). However, the fact that they are half-bond means they exhibit particular stress-dependent behavior reminiscent of unbound granular materials [8,9]. For this reason, many researchers have found it interesting to study CRMs using triaxial tests with different confining pressures [3,10–12]. The triaxial test results

* Corresponding author.
E-mail addresses: porosaig@purdue.edu, p.orosa@udc.es (P. Orosa), iperez@udc.es (I. Pérez), arodriguezpa@udc.es (A.R. Pasandín), jhaddock@purdue.edu (J.E. Haddock).

https://doi.org/10.1016/j.conbuildmat.2023.131439
Received 24 January 2023; Received in revised form 23 March 2023; Accepted 12 April 2023
Available online 21 April 2023

allow for fitting to nonlinear behavioral models, typically used for granular materials, and implementing such models in numerical simulation software [13–15]. There are investigations on the evolution of the nonlinear behavior of CRM with curing [2,16], but most of them focus on the stress-dependent nonlinear behavior [17], or the temperature- and frequency-dependent behavior [18]. However, a few have examined the nonlinear and temperature-dependent mechanical behavior together [19].

2. Aims and scope

CRM are known to exhibit time-, temperature-, and stress-dependent mechanical behavior. Many researchers have studied these behaviors separately, but analyses of the combined response are limited. This study performed dynamic triaxial (DTx) tests with different confinement levels (ranging from 20 to 200 kPa) at various temperatures (5, 15, 25, and 35 °C) on three different CRM.

The CRM were prepared with a Superpave Gyratory Compactor (SGC), reaching an air void target level during compaction. The first CRM, considered the control mixture, was comprised of 100% RAP and 3.3% bitumen emulsion (by total aggregate mass), with no active filler addition. The second CRM incorporated 1% Portland cement (C) to the control mixture, and the third CRM added 1% hydrated lime (HL) to the control, which allowed for the assessment of the active filler effect on the temperature- and stress-dependent behavior of CRM.

Finally, applying the principle of superposition to the variables of temperature and stress level, master curves of the resilient moduli for the three mixtures were plotted and compared.

3. Materials

The solid phase of the CRM studied in this research was mainly composed of RAP, provided by a local paving contractor in Lafayette, Indiana, USA. The RAP maximum size is 12.7 mm. Fig. 2 illustrates its grain size distribution and the 0.45 power maximum density curve. The average bitumen content of the RAP was 3.90 percent.

An anionic bitumen emulsion, type SS-1, with a residual binder content of 62%, was used for all the CRM prepared. Based on CRM recommendations and previous experience [7,21], the prepared mixtures incorporated a fixed proportion of 3.2% bitumen emulsion (BE), corresponding to 2.0% residual binder. A 2.5% water content (W) was added to improve mixing and compaction in all the CRM. Furthermore, to enhance the mechanical properties of the studied CRM, the addition of 1% active fillers was considered. The active fillers were Portland cement (C) and hydrated lime (HL). Table 1 displays the details of the mixture designs for the three different CRM.

4. Methods

4.1. Specimen preparation

The CRM specimens were compacted at room temperature using a SGC (Fig. 3a). Given that the volumetric properties in terms of air void contents are a fundamental parameter for mechanical properties [22–24], it was decided to use a compaction energy that would guarantee the same air voids content (V_a) in all the CRM. Fixing V_a in the CRM studied avoids the effects of different volumetric properties on the mechanical properties investigated and facilitates analyzing the effect of the different types of filler used. The target V_a was set at 15%, based on values obtained in previous investigations and consulted field reports

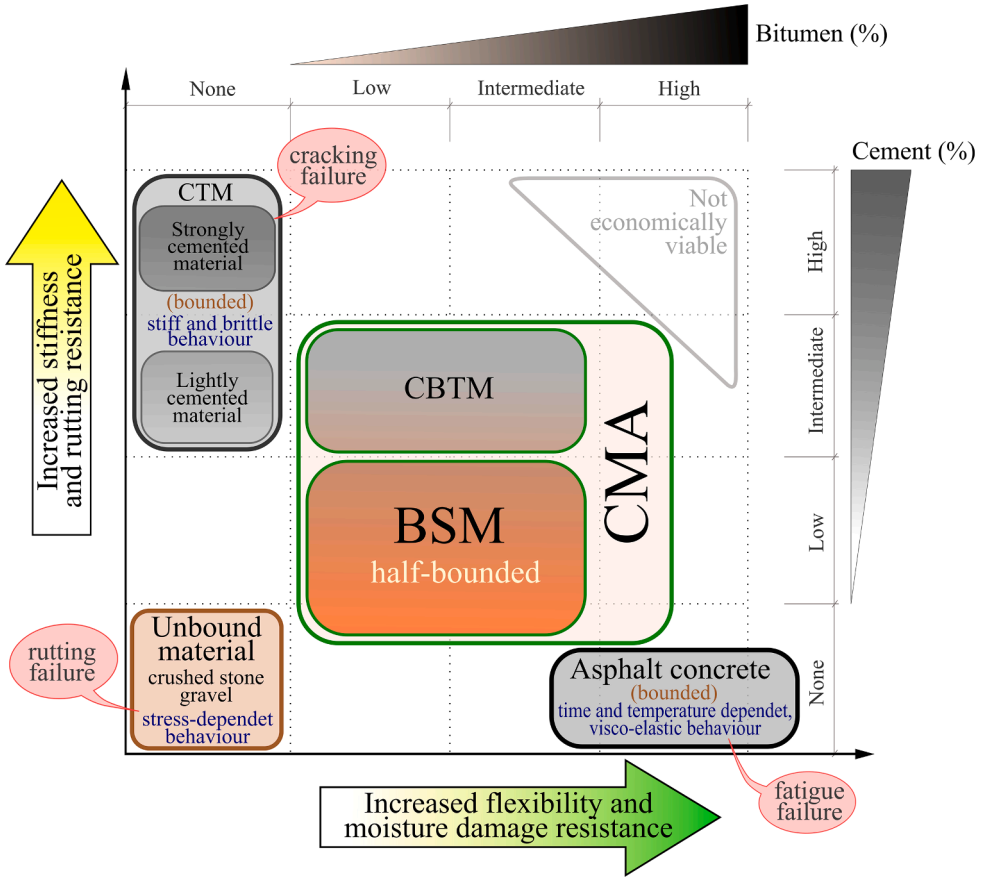

Fig. 1. Conceptual behavior of pavement materials as a function of bitumen and cement contents [20].

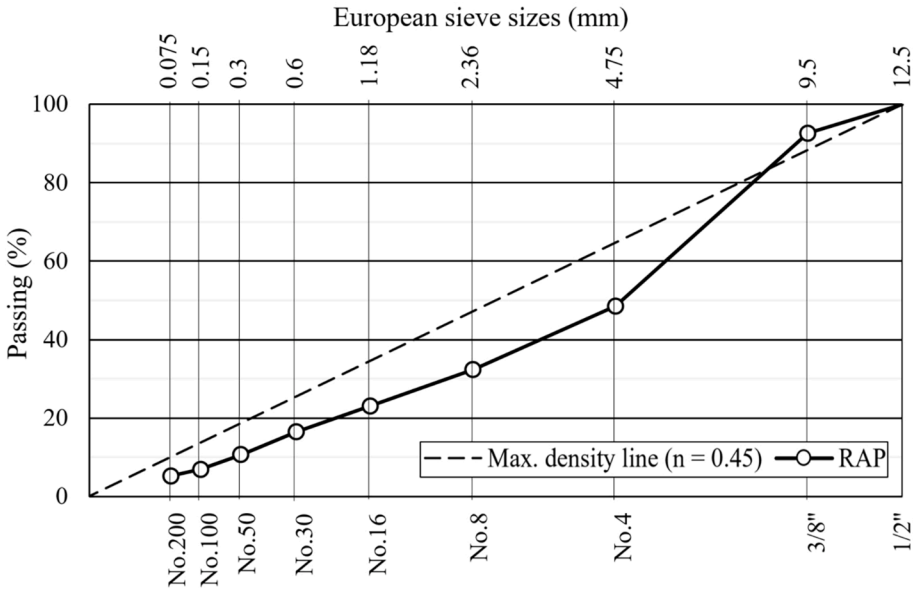

Fig. 2. RAP gradation.

Table 1
Mixture design proportions and maximum densities.

Mixture	RAP (%)	C (%)	HL (%)	BE (%)	W (%)	G_{mm} (g/cm^3)
CRM–0	100	0	0	3.2	2.5	2.475
CRM–C	100	1	0	3.2	2.5	2.483
CRM–HL	100	0	1	3.2	2.5	2.487

[25]. Three specimens of each mixture were prepared.

The specimens needed to be 100 mm in diameter and 150 mm in height due to the requirements of the triaxial equipment. Therefore, specimens of 150 mm in height and diameter were produced, and after being cured, 100 mm diameter cores were extracted (Fig. 3b). The selected curing for all the CRM was at 40 °C in a forced draft oven for three days, as proposed by Asphalt Academy Technical Guideline [7] and supported by previous scholars [20,26,27].

4.2. Volumetric properties

The maximum densities (G_{mm}) of the three mixtures studied were obtained by the CoreLok method, which was necessary to establish the required compaction to a fixed level of V_a. The CoreLok procedure requires a dry mix sample to be placed inside a vacuum bag and sealed inside the CoreLok vacuum chamber. The bag is opened underwater, determining the immersed weight. Finally, the G_{mm} results from the weight in air and the immersed weight (ASTM D6857). The obtained maximum densities are shown in Table 1.

Based on the gyratory compactor data, the bulk densities of the 150 × 150 mm specimens were obtained after compaction but before curing ($G_{mb,0}$) using the dimensional method (DM) based on mass and measurements (AASHTO T312). The compaction evolution with the number of gyrations was also analyzed regarding density and air voids content ($G_{mb,0}$, and $V_{a,0}$, respectively). After curing, the bulk densities were again obtained for the 150 × 150 mm specimens ($G_{mb,150}$) and the 100 mm diameter cores ($G_{mb,100}$), using the dimensional and SSD methods (AASHTO T166).

4.3. Dynamic triaxial tests at different temperatures

All the DTx tests were performed on the prepared CRM using a B200L Asphalt Mixture Performance Tester (AMPT) provided by Pavetest (Matest). The AMPT is a computer-controlled hydraulic testing machine that subjects an asphalt mixture specimen to confining pressure, different temperatures inside a removable chamber, and various cyclic axial loading frequency ranges (Fig. 4).

To apply adequate confining pressure to the CRM specimens, they

Fig. 3. (a) Gyratory compaction of a 150 mm diameter specimen, (b) extraction of 100 mm diameter cores.

were placed inside elastic membranes, which were sealed using O-rings on the upper and lower platens (Fig. 4). The deformations were recorded through 3 strain gauge transducers, placed in the middle third of the specimen, and magnetically attached through previously glued pieces.

The AMPT was programmed to perform a DTx test with different constant confining pressures (CCP), σ_3, ranging from 20 to 200 kPa, with different levels of cyclic deviatoric stress, σ_d. The σ_d values present a sinusoidal shape variation between $\sigma_{d,\min}$ (equal to zero in all the loading sequences) and $\sigma_{d,\max}$, listed in Table 2. Thirty-four loading sequences of 100 cycles were used, after an initial conditioning sequence of 250 cycles, as summarized in Table 2.

The first 29 load sequences were adopted from the EN 13286-7 standard, used for calculating *Mr* in granular materials for base courses. However, since the test was performed on bituminous mixtures, it was decided to add 5 additional sequences, following the same pattern, which allowed for examining higher stress states. Throughout the test, for each loading cycle, it was possible to calculate the resilient modulus (*Mr*) as the relation between the applied deviatoric stress, σ_d, and the resilient or elastic deformation, ε_r, measured in a given loading cycle, as shown in Equation (1). In compliance with the EN standard, the frequency used was a constant 1 Hz.

$$M_r = \frac{\sigma_d}{\varepsilon_r} \tag{1}$$

where σ_d was calculated as the difference between the maximum or principal stress applied, σ_1, and the confining pressure, σ_3. Table 2 displays the maximum and minimum values of σ_d.

In addition to the indications of the standard test method, it was decided to perform testing at different temperatures to consider the influence of this parameter on the mechanical behavior of CRM. Thus, the test described above was performed at 5, 15, 25, and 35 °C. The CRM specimens were prepared for testing by spending at least 4 h in a climatic chamber at the appropriate temperature. The AMPT was set up so the triaxial chamber would maintain this temperature.

Table 2
Applied load sequences, adapted from EN 13286–7.

Sequence	σ_3 (kPa)	$\sigma_{d,\ \max}$ (kPa)	$\theta = \sigma_1 + 2\sigma_3$ (kPa)
Conditioning	70	200	410
1	20	30	90
2	20	50	110
3	20	80	140
4	20	115	175
5	35	50	155
6	35	80	185
7	35	115	220
8	35	150	255
9	35	200	305
10	50	80	230
11	50	115	265
12	50	150	300
13	50	200	350
14	50	280	430
15	70	115	325
16	70	150	360
17	70	200	410
18	70	280	490
19	70	340	550
20	100	150	450
21	100	200	500
22	100	280	580
23	100	340	640
24	100	400	700
25	150	200	650
26	150	280	730
27	150	340	790
28	150	400	850
29	150	475	925
30	200	280	880
31	200	340	940
32	200	400	1000
33	200	475	1075
34	200	550	1150

Note: $\sigma_{d,\ \min}$ is equal to zero in all the load sequences.

4.4 Numerical prediction models of the resilient modulus

Several nonlinear models have been proposed to reproduce the behavior of unbound granular materials with stress-dependent behavior. One of the simplest and most widely known and employed is the *k-θ* model, proposed by Hicks [28]. This model describes the resilient modulus in terms of the sum of principal stresses, known as bulk stress or the first stress invariant, $\theta = \sigma_1 + 2\sigma_3$, as:

$$M_r = k_1 \cdot \theta^{\ k_2} \tag{2}$$

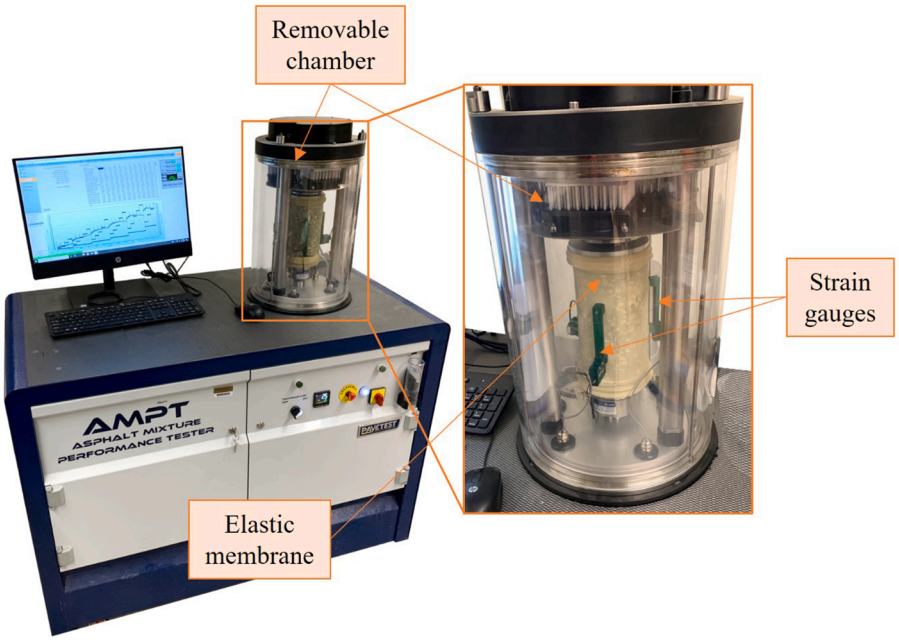

Fig. 4. AMPT device used, with detail of CRM specimen inside latex membrane with LVDT arrangement, placed inside a triaxial chamber.

where k_1 and k_2 are constants of the material. The model may, however, oversimplify the relationship between stress and strain in many situations, because most of the elastic moduli of pavements and unbound materials depend on the total stress and the degree of shear deformation. In this research, the simplicity of the Hicks model allowed simple graphical comparisons of the experimental results, since it provides their potential regression.

4.5. Adaptation of the time–temperature superposition principle to the stress–dependent nonlinear mechanical behavior

The Time-Temperature Superposition Principle (TTSP) is validated in the linear and nonlinear domains for most bituminous materials [29,30]. As a result, master curves can be generated at a single reference temperature (T_{ref}) by shifting experimental data on the frequency axis. The present study analyzes the nonlinear mechanical behavior of CRM in terms of temperature and stress level, and a similar approach to the TTSP is proposed based on the resilient modulus results from the experiment.

Using the proposed Stress-Temperature Superposition Principle (STSP), the master curves, Mr^*, in MPa, were generated by shifting the axis corresponding to the stress data in terms of the bulk stress, θ, in kPa. The shifted bulk stresses are denoted as reduced stresses (θ_{red}), which are the bulk stresses of the other temperatures (θ_T) multiplied by shift factors (a_T) that depend on the temperature T, in K:

$$\theta_{red} = a_T(T)\cdot\theta_T \tag{3}$$

In the proposed STSP, the variation of the shift factors with temperature can be expressed using the Williams–Landel–Ferry (WLF) equation [31], also used in the TTSP [32]:

$$\log(a_T) = -\frac{C_1\left(T - T_{ref}\right)}{C_2 + T - T_{ref}} \tag{4}$$

where C1 and C2 are the constants of the WLF equation, and *Tref* is the reference temperature. Thus, the master curves, Mr^*, were obtained using the following equation (5):

$$\log(Mr^*) = \delta + \frac{\alpha}{1 + e^{\beta+\gamma\cdot\log\left(\frac{1}{\theta_r}\right)}} \tag{5}$$

where α, β, δ, ɣ are coefficients of the material. These coefficients, as well as C1 and C2, were obtained by regression, minimizing the total square error.

5. Results and discussion

5.1. Volumetric properties

All CRM specimens were compacted with SGC until obtaining a V_a of 15 percent. Fig. 5 shows the compaction curves resulting from the SGC recording. It can be observed that the addition of filler facilitated compaction, reaching the target voids for a lower number of compaction gyrations. This reduction of gyrations was more evident in the mixture with cement than with hydrated lime. The representation of the standard deviations shows that the CRM with cement also showed the greatest variability.

Table 3 summarizes the measured volumetric properties (bulk density and air voids content) of the 150 × 150 mm specimens before and after curing ($G_{mb,0}$ and $V_{a,0}$ before curing, and $G_{mb,150}$ and $V_{a,150}$ after curing), as well as after curing for the 100 × 150 mm specimens ($G_{mb,100,}$ and $V_{a,100}$). Table 3 also indicates the range of required compaction gyrations (N_{SGC}) to achieve the target compaction in each CRM.

Density reduction due to water evaporation after curing can be easily identified from Table 3 in all cases. Comparing the results by DM or SSD method, the densities by SSD method were always higher. This result was already reported in previous studies of volumetric properties for CRM, explained due to the high porosity of this material. During the saturated dry surface weight measurement, it is easy for water to drain from the pores, resulting in the measurement of higher density values. Therefore, this method is not recommended for mixtures with high porosity.

Comparing the results of the 150 mm specimens with the 100 mm specimens showed a general increase in the densities after coring. These results are logical since it is an internal portion of the specimen. The compaction is assumed to be more severe in the specimen's interior, so the air voids content of the 100 mm cores is lower than the 150 mm initial specimens.

Analyzing the number of required gyrations, N_{SGC}, and the compaction curves in Fig. 5, adding filler to the CRM appears to improve (facilitate) compaction. Consequently, less energy (lower N_{SGC}) was required to obtain similar volumetric properties after compaction ($G_{mb,0}$). A greater filling of the voids in the mixture and the interstitial effect of these fillers during hydration could explain this result. Considering the filler as part of the mineral skeleton, it fills the voids between coarse and fine aggregates, thus sealing and densifying the mixture and increasing the stability of the whole. Ultimately, the filler can facilitate compaction, acting as a lubricating element between the coarser aggregates, and can make the mixture more workable by

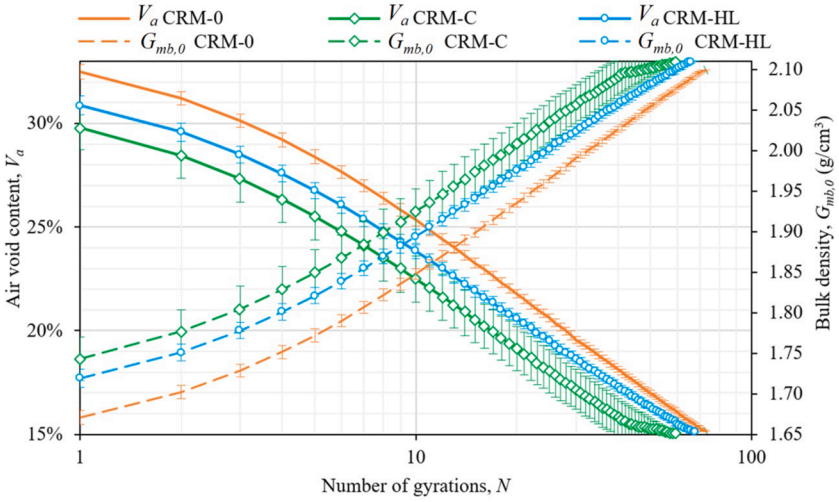

Fig. 5. CRM compaction curves.

Table 3
Average volumetric properties (bulk densities in g/cm^3, and air voids content in %) obtained using the dimensional method (DM) and SSD method for the different CRM.

	$G_{mb,0}$	$G_{mb,150}$		$G_{mb,100}$		$V_{a,0}$	$V_{a,150}$		$V_{a,100}$	
	DM	DM	SSD	DM	SSD	DM	DM	SSD	DM	SSD
CRM–0	2.100	2.046	2.082	2.085	2.125	0.151	0.173	0.159	0.157	0.141
N_{SGC} = 71–73										
CRM–C	2.110	2.053	2.089	2.088	2.132	0.151	0.173	0.159	0.159	0.141
N_{SGC} = 42–59										
CRM–HL	2.110	2.052	2.090	2.077	2.125	0.152	0.175	0.160	0.165	0.145
N_{SGC} = 64–68										

enveloping the coarse aggregates and preventing their segregation [33,34]. This effect was more pronounced in the case of cement addition than when using hydrated lime.

5.2. Effect of temperature on the stress-dependent mechanical behavior of CRM

As a result of the DTx tests, the nonlinear and stress-dependent *Mr* is measured. Throughout the test, the stress level increase leads to an increase in the *Mr*. The markers in Fig. 6 show the experimental *Mr* results obtained from the DTx tests conducted on the control mixture, CRM–0, at the four temperatures considered. The graph in Fig. 6 also shows the potential regression of the results at each temperature, corresponding with the Hicks predictive model (*k-θ* model). The fitted parameters of this model for the CRM–0 mixture are shown in Table 5.

Since the CRM are an asphalt material, a meaningful increase in *Mr* values was observed with decreasing temperature (Fig. 6). From the maximum *Mr* (*maxMr*) and minimum *Mr* (*minMr*) values obtained in the DTx, two parameters were derived to facilitate the analysis of the results. First, the average slope of the *Mr* variation with θ (*SMr*) was obtained as $SMr = (maxMr - minMr)/(max\theta - min\theta)$, with maxθ and minθ being the maximum and minimum values of θ during the DTx tests, respectively. Second, the percentage variation of *Mr* (ΔMr) was obtained as $\Delta Mr = (maxMr - minMr)/minMr$. These parameters, corresponding to mixture CRM–0, are shown in the first four rows of Table 4.

From the calculated parameters (Table 4), it can be observed that with increasing temperatures, there is a reduction in the slope value *SMr*. This outcome means that the increase in temperature makes the *Mr* of CRM–0 more stable than that obtained at colder temperatures and, consequently, less sensitive to the increase in the stress level. However, considering the percentage increase of *Mr* (ΔMr), the opposite occurred. The DTx at higher temperatures showed higher percentage increases between the *minMr* and *maxMr*. Thus, in the case at 35 °C, the *maxMr* is more than twice the *minMr*, showing an increase of 113.40 percent.

Table 4
Minimum and maximum resilient modulus obtained in the DTx at different temperatures for the three CRM, average slope (*SMr*), and percentage increase of *Mr* (ΔMr).

		5 °C	15 °C	25 °C	35 °C
CRM–0	*minMr*	2388.01	1720.22	1325.80	941.08
	maxMr	4431.86	3281.47	2604.80	2008.30
	SMr	1.93	1.47	1.21	1.01
	ΔMr	85.59%	90.76%	96.47%	113.40%
CRM–C	*minMr*	4460.30	2953.80	1910.50	1457.61
	maxMr	6048.61	4501.22	3125.11	2921.28
	SMr	1.50	1.46	1.15	1.49
	ΔMr	35.61%	52.39%	63.58%	100.41%
CRM–HL	*minMr*	5704.47	3129.41	1765.15	1650.02
	maxMr	7313.79	4655.12	2975.12	2965.18
	SMr	1.52	1.44	1.14	1.24
	ΔMr	28.21%	48.75%	68.55%	79.71%

Table 5
Fitted constants of the *k–θ* model (k_1, and k_2), and its quadratic square error (R^2), for the three CRM at the different considered temperatures.

		k_1	k_2	R^2
CRM–0	5 °C	673.78	0.2701	0.9665
	15 °C	435.44	0.2879	0.9396
	25 °C	366.60	0.2812	0.9474
	35 °C	236.74	0.3114	0.9341
CRM–C	5 °C	2471.50	0.1257	0.9684
	15 °C	1244.80	0.1825	0.9490
	25 °C	730.56	0.2076	0.9380
	35 °C	379.29	0.2958	0.9312
CRM–HL	5 °C	3837.10	0.0930	0.9704
	15 °C	1348.20	0.1772	0.9481
	25 °C	618.70	0.2234	0.9314
	35 °C	568.90	0.2335	0.9282

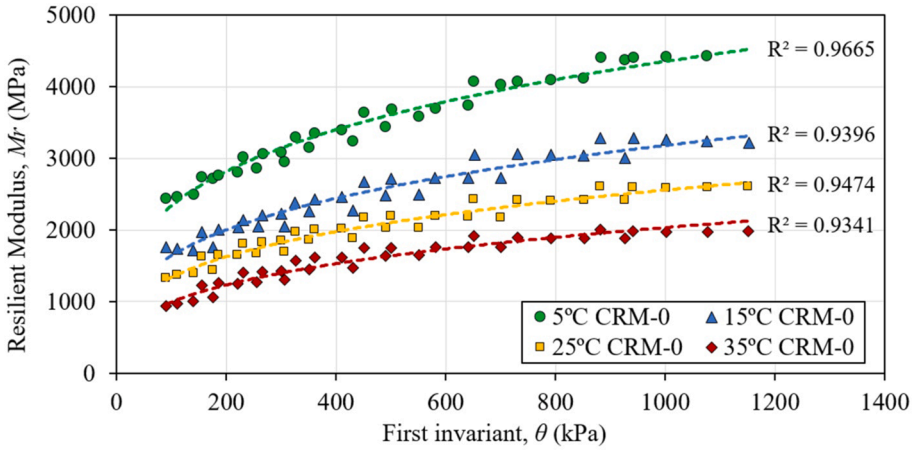

Fig. 6. Resilient modulus obtained from the DTx tests of CRM–0 at the different temperatures, and representation of the fitted potential k–θ model.

However, in the case of the lowest considered temperature (5 °C), *ΔMr* is also substantial, but to a minor extent (85.59%). Therefore, it can be clearly stated that the stiffness variation, in this case of the *Sr*, of the CRM-0 mixture depends logically on the temperature and meaningfully on the stress level (stress-dependent behavior). The obtained trend can be explained by the viscoelastic behavior of asphalt, which makes it softer and less viscous at higher temperatures. This makes asphalt mixtures resist more due to their mineral skeleton than the cohesion of the mastic at higher temperatures. Thus, the stress and confinement level sensitivity is more evident under these conditions, similar to a granular material without a binder.

5.3. Effect of active filler addition on the stress-dependent mechanical behavior of CRM

The addition of active filler in CRM is typically used to improve its mechanical properties, such as stiffness. The DTx results at different temperatures for mixtures CRM–C and CRM–HL, with 1% cement and 1% hydrated lime, respectively, are illustrated in the graphs in Fig. 7. Again, in addition to the experimental results represented by markers, the potential regressions corresponding to the Hicks predictive model are plotted. The fitted parameters of this model are given in Table 5.

The graphs in Fig. 7 show the substantial increase in *Mr* at all temperatures in the CRM-C and CRM-HL mixtures compared to CRM–0 (Fig. 6) because of the active filler addition. This increase is more relevant in the CRM–HL mixture at the lowest studied temperature of 5 °C than in the CRM–C, while in the remaining studied temperatures, the differences between CRM–C and CRM–HL *Mr* values are not so substantial. These differences can be seen in Fig. 8, where, at the respective temperatures, the plots of *Mr* as a function of the first stress invariant, θ, are presented for the three CRM. In addition, Table 4 also summarizes the parameters *minMr*, *maxMr*, *SMr*, and *ΔMr,* for mixtures CRM–C and CRM–HL.

In view of Table 4, the decreasing trend of *SMr* with increasing temperature in the CRM–0 mixture is repeated for the CRM–C and CRM–HL mixtures, but the variation is lower this time. It can be noted that there is a more noticeable decrease in this *SMr* parameter at 25 °C, with no apparent reason.

The variation of *Mr*, *ΔMr* shows an increasing trend, as was the case with the CRM–0 mixture, but considering CRM–C and CRM–HL results, these increases are considerably smaller (Table 4). While in the CRM–0 mixture, increases ranged from 85.59% to 113.40%, in the CRM–C mixture, increases are lower, from 35.61% to 100.41%, and they are even lower for the CRM–HL mixture, ranging from 28.21% to 79.71 percent. All this indicates that after adding active filler, either cement or hydrated lime, the variation of *Mr* with respect to the variation of the stress state is reduced, making the material clearly less stress-dependent. This decrease in stress dependence is more evident with the use of hydrated lime than cement. The use of 1% of hydrated lime in the CRM with 100% RAP led, in general, to a material with higher stiffness values and less stress dependency.

Looking at the same parameter of variation, *ΔMr*, Table 4 shows that in mixtures CRM–C and CRM–HL, the growth of *ΔMr* with increasing temperature from 5 to 25 °C is relatively constant, while there is a more pronounced growth from 25 to 35 °C. This change can also be perceived in the CRM–0 mixture, although it was not as pronounced. As the temperature increases, the binder of the mixture softens and loses cohesive power. At this point, the mineral skeleton of the material becomes more responsible for the bearing capacity of the mixture. Therefore, the behavior becomes more similar to that of an unbound granular material, with greater dependence on the confinement stress to which it is subjected. This characteristic is repeated in all three mixtures, with or without the addition of active fillers, since it is a feature of cold asphalt mixtures.

A conclusion drawn from the values in Table 4 is that adding the studied active fillers reduced the stress dependency and the *ΔMr* values at the respective temperatures compared to the control mixture without filler additions. However, considering the values at 35 °C, the mixture with cement, CRM–C, presents a variation *ΔMr* of 100.41%, similar to those *ΔMr* presented by the CRM–0 mixture. The low addition of Portland cement (1%) did not cause sufficient cementation of the CRM to make it behave as a cementitious material (independent of σ_3). In fact, CRM-C showed a more stress-dependent behavior compared to CRM-HL, as was also reported by other authors [35]. Since 35 °C is a temperature easily reached in the pavement, it is concluded that cement addition is likely less effective in inhibiting stress dependency CRM pavements at higher temperatures.

In contrast, adding hydrated lime was more successful if the objective was to make the CRM stiffer and less dependent on σ_3, presenting a more purely viscoelastic behavior. The improved adhesion between asphalt binder and aggregates provided by the HL could be the reason for this result. Under the effect of HL, the surface of the aggregates becomes basic, generating attraction for the slightly acid radicals of the bitumen, thus favoring bitumen-aggregate adhesion [33,35–37].

Another explanation for the higher *Mr* experienced by CRM-HL could be the larger surface area and low bulk density of the HL. These characteristics make HL a filler with high binder demand, making the bitumen more viscous than using other types of fillers. This stiffens the CRM, improving the plastic deformation resistance [34,38,39]. However, further investigation is necessary on the interaction between the

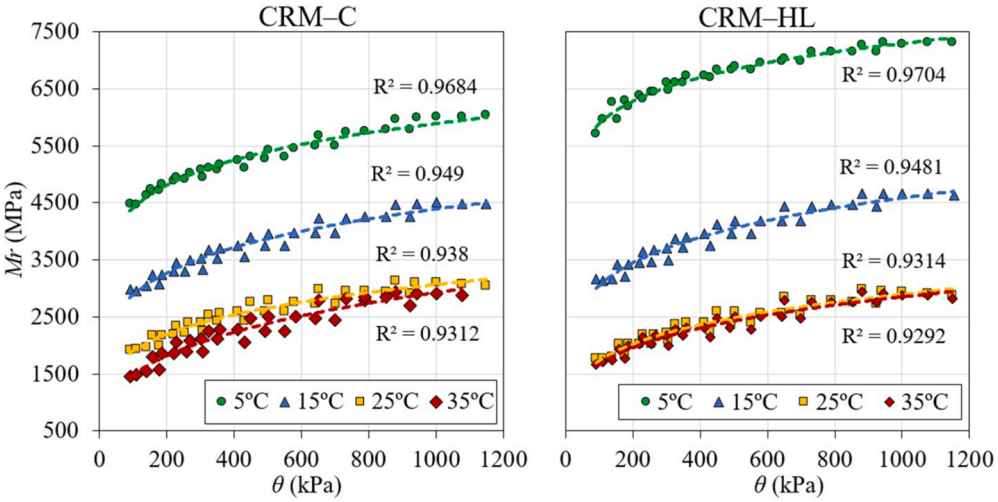

Fig. 7. Resilient modulus obtained from the DTx tests of CRM–C and CRM–HL at the different temperatures, and representation of the fitted potential k–θ model.

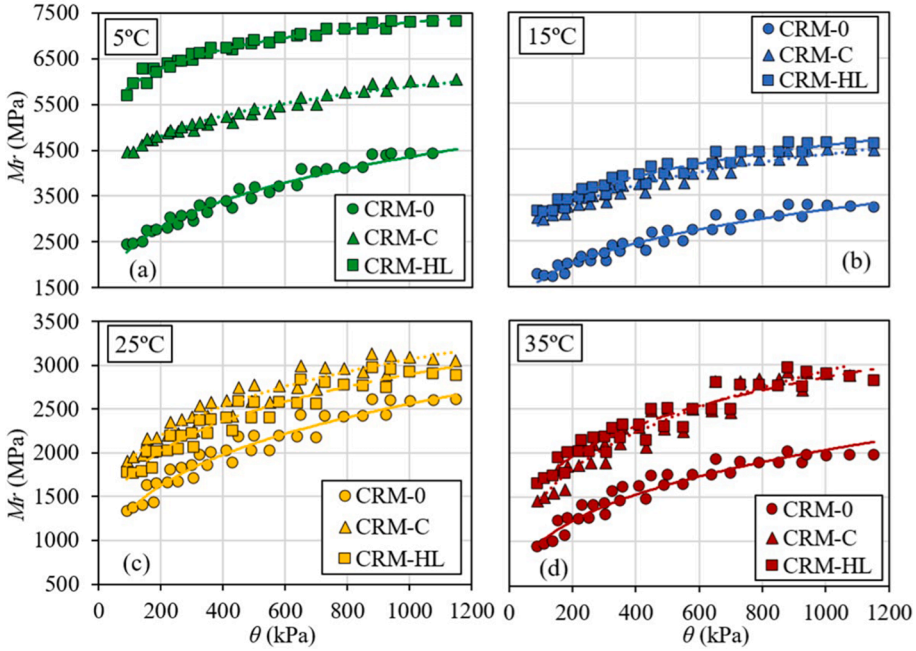

Fig. 8. Comparison of the resilient moduli of the three CRM at each tested temperature: (a) 5 °C, (b) 15 °C, (c) 25 °C, (d) 35 °C.

HL, the aged RAP binder, and even the new binder from the bituminous emulsion.

Table 5 shows the adjusted parameters of the Hicks model mentioned above (2) for the three CRM mixes studied. It is possible to implement this model in numerical simulation software to conduct pavement predictions considering the materials' viscoelastic and stress-dependent mechanical behavior. This simulation software allows for conducting stress and deformational analysis of pavement sections. Combining such software with permanent deformation prediction models capable of estimating rutting [9,11] can be a potent complementary tool in pavement design.

5.4. Stress-temperature superposition approach

The master curves obtained after applying the described STSP approach are shown in Fig. 9 for the three studied CRM at the reference temperature of 15 °C. The different markers refer to each mixture, and the colors refer to each temperature. These curves show the variation of Mr^* with the shifted bulk stress (3), and the adjusted parameters employed in the proposed model are summarized in Table 6.

Several conclusions can be drawn from the master curves in Fig. 9, as analyzed in previous sections. First, it is evident the CRM–0 mixture always has lower Mr^* than do the mixtures with active filler addition,

Table 6
Fitted coefficients C_1 and C_2 of the WLF equation, and material constants used in the Mr^* equation.

	C_1	C_2	α	β	δ	ɣ
CRM–0	5.725	139.767	5.61196	0.00000	2.80734	0.22065
CRM–C	4.0879	57.9041	12.0437	0.0000	0.0003	0.0677
CRM–HL	3.1549	31.4415	12.17049	0.00002	0.00028	0.06032

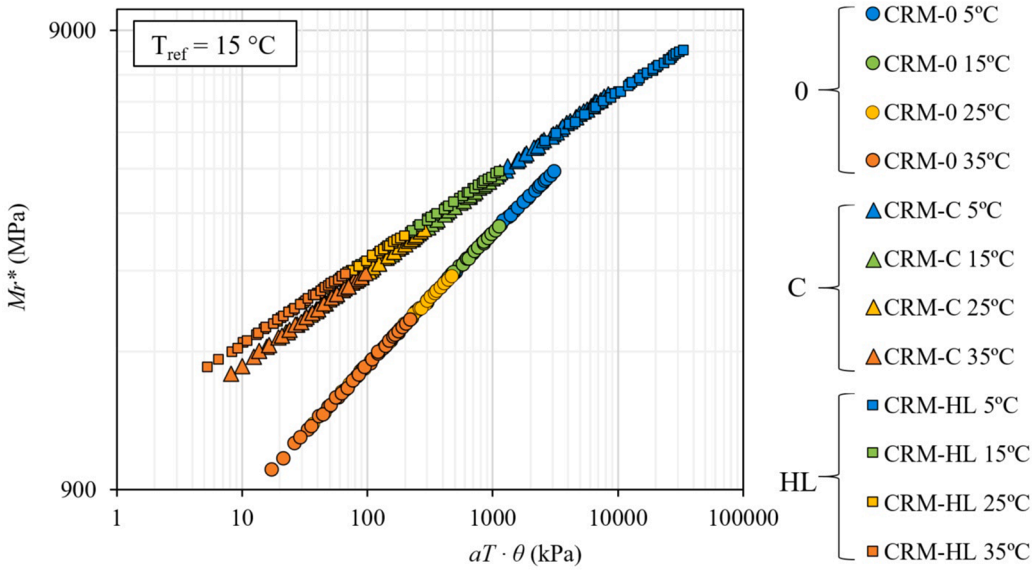

Fig. 9. Master curves of the three CRM and regression parameters at the reference temperature of 15 °C.

CRM–C and CRM–H, at every temperature and stress condition. Comparing the results of CRM–C and CRM–H, the results are in both cases somewhat similar, but CRM–HL always has slightly higher values, and mainly at the lowest temperatures (5 °C), the *Mr** values reached by CRM–HL are the highest, with the most substantial difference compared to CRM–C.

Analyzing the slopes (Fig. 9), similar conclusions to those drawn earlier are obtained. The slope of CRM–0 is much higher, showing a much more stress-dependent behavior. However, mixtures with active filler addition reduce this slope, thus becoming less stress-dependent. As already discussed, this stress dependency reduction is more noticeable in the CRM–HL mixture, which shows the most horizontal slope. Therefore, hydrated lime addition showed a greater increase in *Mr** and a more substantial reduction of stress dependency than cement addition, compared with moduli of the mixture without filler. As already discussed, CRM–C still shows stress-dependent mechanical behavior, given the low cement proportion used.

Consequently, after applying the proposed STSP, the conclusions extracted from the analysis of the master curves in Fig. 9 are analogous to those extracted from the previous extensive analysis but much more straightforward and shorter. For this reason, analyzing cold mixtures' temperature- and stress-dependent behavior using this approach is considered a technique with great interest and potential applications. Additionally, in Fig. 10, the results of *Mr* and the equivalent *Mr** are shown together to illustrate the method's goodness of fit. These plots show a good fit, especially for the CRM–0 mixture.

Overall, along with the viscoelastic nature, the mechanical behavior of cold asphalt mixtures showed a fundamental dependence on the confinement level. Therefore, this proposed novel approach could enhance the understanding of this material, facilitate its study, and collaborate in expanding its use. However, further research and experimentation are undoubtedly necessary to verify its effectiveness and adequacy as a support tool in pavement design.

6. Conclusions

This investigation evaluated the influence of active filler addition of two types (cement and hydrated lime) in cold recycled mixtures (CRM) containing 100% RAP and bitumen emulsion. The effect on the compactability and volumetric properties, as well as on the stress-dependent mechanical behavior, was evaluated. Three different mixtures were manufactured, one with 100% RAP and no active filler addition (CRM–0), one with 1% Portland cement (CRM–C), and one with 1% hydrated lime (CRM–HL), by using a Superpave Gyratory Compactor (SGC). Dynamic triaxial tests with different confinement levels and at four different temperatures (5, 15, 25, and 35 °C) were conducted to evaluate the temperature- and stress-dependent resilient modulus (*Mr*). Finally, a new approach was proposed to analyze the temperature- and stress-dependent mechanical behavior of the CRM, named Stress-Temperature Superposition Principle (STSP), which allowed for obtaining master curves. The conclusions drawn from the study are summarized as follows:

- Filler addition improved the compactability of CRM. CRM–C and CRM–HL mixtures reached the target air voids level with fewer SGC gyrations than the CRM–0 mixture. Cement proved to be the more efficient filler to do this, with CRM–C mixture requiring less compaction energy than the remaining two mixtures. This effect was attributed to the increased void filling and the interstitial effect of cement during hydration.
- Increasing temperatures showed a decrease of maximum and minimum *Mr* values during the dynamic triaxial tests and increased stress dependency (more substantial variation of *Mr* with the increasing stress level).
- The active filler addition showed two evident effects: on the one hand, it considerably increased *Mr* values, and on the other hand, it reduced the dependence of *Mr* on the stress level, at all temperatures studied, compared with the control mixture. Both effects were more noticeable when the filler used was hydrated lime, showing higher *Mr* and lower variations. This result was attributed to improved adhesion between the asphalt binder and the RAP and the greater surface area of this filler.
- The master curves plotted according to the proposed STSP made it possible to use a single graph to analyze all the results. The conclusions drawn were equivalent but in a much simpler way. Thus, this analysis methodology offers a powerful tool for studying the temperature- and stress-dependent behavior of cold asphalt mixtures.

Adding a small amount of active filler in CRM has proven to greatly affect compactability and volumetric and mechanical properties. Future research aims to explore different filler dosages and alternatives, and the interactions of those with the aged binder of the RAP, if any. Nowadays, many industrial wastes or by-products in filler form could present chemical activity and potentially have an interesting effect when applied in cold bituminous recycled mixtures.

Regarding the mechanical behavior, the evolution of *Mr* was studied at different stress states and temperatures, but it is also a subject of future research to implement the frequency variable. It is important to note that, given the evident mechanical behavior dependent on σ_3, it should be kept in mind that tests such as dynamic modulus, without consideration of confining stresses, could underestimate the stiffness of cold asphalt mixtures. In addition, tests on completely cured CRM could

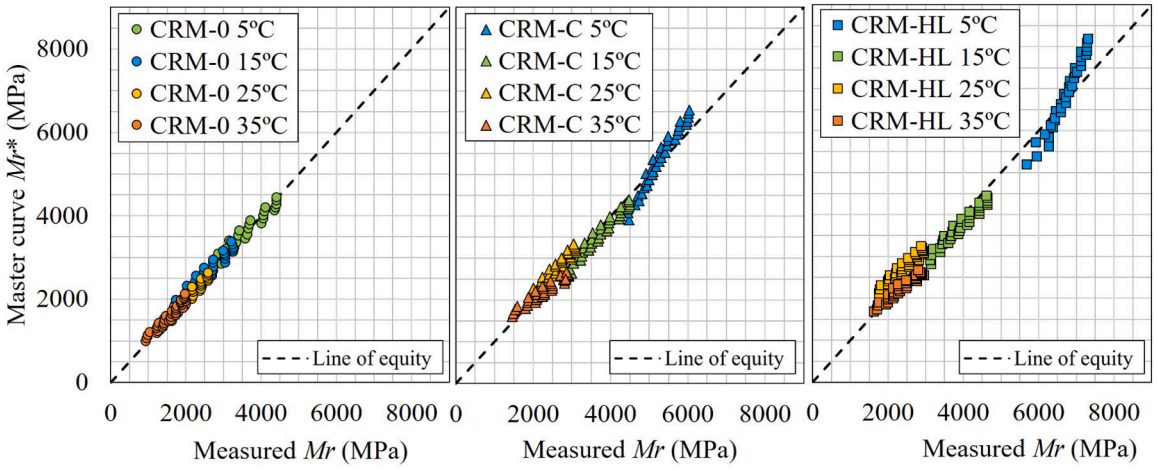

Fig. 10. Measured *Mr* versus master curve *Mr**.

overestimate the stiffness results obtained since they do not consider the possible remanent water in the mixtures. Thus, it would be of great interest to evaluate this particular mechanical behavior at different curing levels and implement the fitted predictive models in numerical simulation of the pavement.

Declaration of Competing Interest

The authors declare that they have no known competing financial interests or personal relationships that could have appeared to influence the work reported in this paper.

Data availability

Data will be made available on request.

Acknowledgments

The authors would like to acknowledge funding for the project BIA2016-80317-R from the Spanish Ministry of Science and Innovation, with an associated pre-doctoral scholarship for the training of research workers (FPI) BES-2017-079633. This scholarship also funded the corresponding author for conducting a pre-doctoral stay in a foreign research center, making it possible to carry out this research study. An special acknowledgement to the Universidade da Coruña/ CISUG for funding part of the Elsevier's open access charge. The authors also acknowledge Milestone Contractors for contributing to the investigation with the recycled materials used. Moreover, finally, the corresponding author would like to express special thanks to Ayesha Shah, Behnam Jahangiri, and Mohammad Ali Notani for their help and support during the laboratory work, and to the rest of the people in the Innovative Materials and Pavements Group, Oscar Moncada, Bongsuk Park, Maya Khajehvand, for their hospitality during the pre-doctoral stay.

References

[1] F.D.B. Albuquerque, M.A. Maraqa, R. Chowdhury, T. Mauga, M. Alzard, Greenhouse gas emissions associated with road transport projects: Current status, benchmarking, and assessment tools, Transp. Res. Procedia. 48 (2020) 2018–2030, https://doi.org/10.1016/j.trpro.2020.08.261.

[2] P. Orosa, I. Pérez, A.R. Pasandín, Short-term resilient behaviour and its evolution with curing in cold in-place recycled asphalt mixtures, Constr. Build. Mater. 323 (2022), 126559, https://doi.org/10.1016/j.conbuildmat.2022.126559.

[3] S. Casillas, A. Braham, Quantifying effects of laboratory curing conditions on workability, compactability, and cohesion gain of cold in-place recycling, Road Mater. Pavement Des. 22 (2021) 2329–2351, https://doi.org/10.1080/14680629.2020.1753101.

[4] B.K. Diefenderfer, D.H. Timm, B.F. Bowers, Structural Study of Cold Central Plant Recycling Sections at the National Center for Asphalt Technology (NCAT) Test Track: Phase II, Virginia, Dept. of Transportation (2019).

[5] B.F. Bowers, B.K. Diefenderfer, G. Wollenhaupt, B. Stanton, I. Boz, Laboratory Properties of a Rejuvenated Cold Recycled Mixture Produced in a Conventional Asphalt Plant. Airf. Highw. Pavements, 2019.

[6] A. Grilli, A. Graziani, E. Bocci, M. Bocci, Volumetric properties and influence of water content on the compactability of cold recycled mixtures, Mater. Struct. 49 (2016) 4349–4362, https://doi.org/10.1617/s11527-016-0792-x.

[7] A. Academy, Technical Guideline (TG2): Bitumen Stabilised Materials Southern African Bitumen Association (Sabita), Pretoria, South Africa, 2020.

[8] L.-J. Ebels, Characterisation of Material Properties and Behaviour of Cold Bituminous Mixtures for Road Pavements, Stellenbosch University, 2008.

[9] I. Pérez, L. Medina, M.Á. del Val, Mechanical properties and behaviour of in situ materials which are stabilised with bitumen emulsion, Road Mater. Pavement Des. 14 (2013) 221–238, https://doi.org/10.1080/14680629.2013.779301.

[10] E. Santagata, G. Chiappinelli, P.P. Riviera, O. Baglieri, Triaxial Testing for the Short Term Evaluation of Cold-Recycled Bituminous Mixtures, Road Mater. Pavement Des. 11 (2010) 123–147, https://doi.org/10.1080/14680629.2010.9690263.

[11] P. Orosa, I. Pérez, A.R. Pasandín, Evaluation of the shear and permanent deformation properties of cold in-place recycled mixtures with bitumen emulsion using triaxial tests, Constr. Build. Mater. 328 (2022), 127054, https://doi.org/10.1016/j.conbuildmat.2022.127054.

[12] B. Gómez-Meijide, I. Pérez, Nonlinear elastic behavior of bitumen emulsion-stabilized materials with C&D waste aggregates, Constr. Build. Mater. 98 (2015) 853–863, https://doi.org/10.1016/j.conbuildmat.2015.07.004.

[13] P. Orosa, L. Medina, J. Fernández-Ruiz, I. Pérez, A.R. Pasandín, Numerical simulation of the stiffness evolution with curing of pavement sections rehabilitated using cold in-place recycling technology, Constr. Build. Mater. 335 (2022), https://doi.org/10.1016/j.conbuildmat.2022.127487.

[14] I. Pérez, L. Medina, M.A. Del Val, Nonlinear elasto-plastic performance prediction of materials stabilized with bitumen emulsion in rural road pavements, Adv. Eng. Softw. 91 (2016) 69–79, https://doi.org/10.1016/j.advengsoft.2015.10.009.

[15] I. Pérez, L. Medina, B. Gómez-Meijide, P.A. Costa, A.S. Cardoso, Numerical simulation of bitumen emulsion-stabilised base course mixtures with C&D waste aggregates considering nonlinear elastic behaviour, Constr. Build. Mater. 249 (2020), https://doi.org/10.1016/j.conbuildmat.2020.118696.

[16] P. Orosa, I. Pérez, A.R. Pasandín, Evaluation of water loss and stiffness increase in cold recycled mixes during curing, Case Stud. Constr. Mater. 18 (2023) e01877.

[17] K.J. Jenkins, F.M. Long, L.-J. Ebels, Foamed bitumen mixes = Shear performance? Int. J. Pavement Eng. 8 (2007) 85–98, https://doi.org/10.1080/10298430601149718.

[18] F. Cardone, A. Grilli, M. Bocci, A. Graziani, Curing and temperature sensitivity of cement-bitumen treated materials, Int. J. Pavement Eng. 16 (2015) 868–880, https://doi.org/10.1080/10298436.2014.966710.

[19] A. Behera, S. Charmot, A. Asif, J.M. Krishnan, Influence of Confinement Pressure on the Mechanical Response of Emulsified Cold-Recycled Mixtures, J. Mater. Civ. Eng. 33 (2021) 1–13, https://doi.org/10.1061/(asce)mt.1943-5533.0003871.

[20] P. Orosa, Mechanical behaviour of cold in-place recycled asphalt mixtures with bitumen emulsion. Effect of curing time on the response of rehabilitated pavement sections, Universidade da Coruña, 2022. http://hdl.handle.net/2183/30989.

[21] P. Orosa, G. Orozco, J.C. Carret, A. Carter, I. Pérez, A.R. Pasandín, Compactability and mechanical properties of cold recycled mixes prepared with different nominal maximum sizes of RAP, Constr. Build. Mater. 339 (2022) 127689.

[22] S. Raschia, C. Mignini, A. Graziani, A. Carter, D. Perraton, M. Vaillancourt, Effect of gradation on volumetric and mechanical properties of cold recycled mixtures (CRM), Road Mater. Pavement Des. 20 (2019) S740–S754. doi: 10.1080/14680629.2019.1633754.

[23] J. Haddock, C. Pan, A. Feng, T.D. White, Effect of Gradation on Asphalt Mixture Performance, Transportation Research Record 1681 (1) (1999) 59–68.

[24] M.R. Pouranian, J.E. Haddock, M. Asce, Effect of Aggregate Gradation on Asphalt Mixture Compaction Parameters, J. Mater. Civ. Eng. 32 (2020) 04020244, https://doi.org/10.1061/(ASCE)MT.1943-5533.0003315.

[25] P. Orosa, A.R. Pasandín, I. Pérez, Compaction and volumetric analysis of cold in-place recycled asphalt mixtures prepared using gyratory, static, and impact procedures, Constr. Build. Mater. 296 (2021) 123620.

[26] A. Graziani, C. Godenzoni, F. Cardone, M. Bocci, Effect of curing on the physical and mechanical properties of cold-recycled bituminous mixtures, Mater. Des. 95 (2016) 358–369, https://doi.org/10.1016/j.matdes.2016.01.094.

[27] J.-P. Serfass, J.-E. Poirier, J.-P. Henrat, X. Carbonneau, Influence of curing on cold mix mechanical performance, Mater. Struct. 37 (5) (2004) 365–368.

[28] R.G. Hicks, Factors influencing the resilient response of granular materials, University of California, Berkeley, 1970.

[29] H.M. Nguyen, S. Pouget, H. Di Benedetto, C. Sauzéat, Time-temperature superposition principle for bituminous mixtures, Eur. J. Environ. Civ. Eng. 13 (2009) 1095–1107, https://doi.org/10.1080/19648189.2009.9693176.

[30] Q.T. Nguyen, H. Di Benedetto, C. Sauzéat, N. Tapsoba, Cédric Sauzéat, Time Temperature Superposition Principle Validation for Bituminous Mixes in the Linear and Nonlinear Domains, J. Mater. Civ. Eng. 25 (9) (2013) 1181–1188.

[31] N.W. Tschoegl, W.G. Knauss, I. Emri, The Effect of Temperature and Pressure on the Mechanical Properties of Thermo-and/or Piezorheologically Simple Polymeric Materials in Thermodynamic Equilibrium-A Critical Review, Mech. Time-Dependent Mater. 6 (2002) 53–99.

[32] D. Ferry, Viscoelastic Properties of Polymers, 3rd ed., New York, NY, USA, 1980.

[33] J. Gallego Medina, Efectos del hidrato de cal como aditivo de mezclas bituminosas, Carreteras, Rev. Técnica La Asoc. Española La Carret. (2002) 68–80.

[34] A. Ruiz Rubio, Filler: conceptos, ensayos y normativa, Carreteras, Rev. Técnica La Asoc. Española La Carret. (2002) 11–26.

[35] J.P.C. Meneses, K. Vasconcelos, L.L.B. Bernucci, Stiffness assessment of cold recycled asphalt mixtures – Aspects related to filler type, stress state, viscoelasticity, and suction, Constr. Build. Mater. 318 (2022), 126003, https://doi.org/10.1016/J.CONBUILDMAT.2021.126003.

[36] D. Lesueur, J. Petit, H.-J. Ritter, The mechanisms of hydrated lime modification of asphalt mixtures: a state-of-the-art review, Road Mater. Pavement Des. 14 (2013) 1–16, https://doi.org/10.1080/14680629.2012.743669.

[37] S. Han, S. Dong, M. Liu, X. Han, Y. Liu, Study on improvement of asphalt adhesion by hydrated lime based on surface free energy method, Constr. Build. Mater. 227 (2019), 116794, https://doi.org/10.1016/J.CONBUILDMAT.2019.116794.

[38] I. Ishai, J. Craus, Effects of Some Aggregate and Filler Characteristics on Behavior and Durability of Asphalt Paving Mixtures, Transp. Res. Rec. J. Transp. Res. Board. 1530 (1996) 75–85, https://doi.org/10.1177/0361198196153000110.

[39] D. Lesueur, A. Teixeira, M.M. Lázaro, D. Andaluz, A. Ruiz, A simple test method in order to assess the effect of mineral fillers on bitumen ageing, Constr. Build. Mater. 117 (2016) 182–189, https://doi.org/10.1016/J.CONBUILDMAT.2016.05.003.